J. Am. Chem. Soc. **2000,** *122,* 12289−12296

Raman Spectroscopy and Atomic Force Microscopy of the Reaction of Sulfuric Acid with Sodium Chloride

Christopher D. Zangmeister and Jeanne E. Pemberton*

Contribution from the Department of Chemistry, University of Arizona, 1306 East University Blvd., Tucson, Arizona 85721

Received April 27, 2000. Revised Manuscript Received October 6, 2000

Abstract: The reaction of NaCl with H_2SO_4 is investigated using Raman spectroscopy, atomic force microscopy (AFM), and gravimetric analysis. Raman spectra are consistent with the formation of $NaHSO_4$ with no evidence for Na_2SO_4. The spectra indicate that the phase of $NaHSO_4$ varies with the amount of H_2O in the H_2SO_4. At low H_2O concentrations, the reaction produces anhydrous β-$NaHSO_4$, which undergoes a phase change to anhydrous α-$NaHSO_4$ over the course of 18 h. At higher H_2O concentrations, anhydrous α-$NaHSO_4$ is formed with small amounts of $NaHSO_4{\cdot}H_2O$. AFM measurements on NaCl (100) show the formation of two distinct types of $NaHSO_4$ structures consistent in shape with α-$NaHSO_4$ and β-$NaHSO_4$. The β-$NaHSO_4$ structures are mobile and move along the NaCl (110) plane until they encounter existing stationary α-$NaHSO_4$ structures whereupon the two forms coalescence to form larger α-$NaHSO_4$ structures. Gravimetry was used to determine the amount of HCl evolved upon exposure to aqueous H_2SO_4 solutions modeling atmospheric aerosols. At low H_2SO_4 concentrations, a large percentage of the HCl formed remains dissolved in the H_2O. These results indicate that for conditions simulating relative humidities above 40%, the fraction of HCl released from this reaction may be as low as 0.40 ± 0.11.

Introduction

The majority of chlorine in the atmosphere exists in the form of reservoir HCl.[1] However, HCl can be transformed to reactive Cl at all levels of the atmosphere. Through reaction with OH in the troposphere, HCl is converted to Cl that can readily abstract hydrogen from volatile organic species to form organic radical species. In the stratosphere, the production and transformation of chlorine-containing species are central to the formation of the ozone hole, since a single Cl can result in the destruction of $\sim 10^5$ ozone molecules before one radical ClO is terminated.[1] Thus, the critical role played by reactive chlorine species in many atmospheric processes delineates the need for a fundamental understanding of the formation and reactivity of HCl at all levels of the terrestrial atmosphere.

Both natural and anthropogenic sources of chlorine exist. One natural source of tropospheric chlorine is gaseous HCl from the reaction of atmospheric alkali halides such as NaCl with NO_x and SO_x species.[2,3] NaCl is added to the troposphere at a rate of $\sim 10^{12}$ kg per year by the evaporation of sea salt aerosols.[4] Many studies have shown a significant chloride deficit of sea salt particles (30−80%) when compared to seawater.[5−8] This deficit has been attributed to reactions with inorganic oxide species that generate volatile chlorine compounds.[5−9]

In addition, NaCl is directly injected into the stratosphere by volcanic eruptions. For example, the El Chichon volcanic eruption generated a plume of ~7 wt % NaCl, and also contained NO_x[10] species and aerosol droplets that were ~80 wt % H_2SO_4.[11] Thus the study of the reaction of concentrated H_2SO_4 solutions with particulate NaCl is relevant to upper level atmospheric chemistry.

Reactions of NaCl with gas-phase species which result in release of HCl are inherently heterogeneous processes. Although many studies of such reactions have been reported in which the loss of gaseous reactants or the production of gaseous products are monitored, far fewer studies have focused on the surface chemistry involved in these reactions.[2,12−14] Of those that have been reported, many rely on the techniques of surface science (e.g. scanning electron microscopy with energy-dispersive X-ray spectroscopy, X-ray photoelectron spectroscopy) which oftentimes require the use of vacuum environments[12,15] that can be marginal models of atmospheric conditions. Elegant studies of reactions on NaCl using FTIR spectroscopy have been performed,[3,13,16] but this approach can suffer from inaccessibility to the low-frequency region of the spectrum

---

* To whom correspondence should be addressed.

(1) Seinfeld, J. H.; Pandis, S. N. *Atmospheric Chemistry and Physics: From Air Pollution to Climate Change*; John Wiley and Sons: New York, 1998; p 180.

(2) Vogt, R.; Finlayson-Pitts, B. J. *J. Phys. Chem.* **1994**, *98*, 3747.

(3) Peters, S. J.; Ewing, G. E. *J. Phys. Chem.* **1996**, *100*, 14093.

(4) Graedel, T. E.; Keene, W. E. *Global Biogeochem. Cycles* **1995**, *9,* 47.

(5) Zhuang, H.; Chan, C. K.; Fang, M.; Wexler, A. S. *Atmos. Environ.* **1999**, *33*, 4223.

(6) Kerminen, V.; Pakkanen, T. A.; Hillamo, R. E. *Atmos. Environ.* **1997**, *31*, 2753.

(7) Harkel, M. J. *Atmos. Environ.* **1997**, *31*, 417.

(8) Kleeman, M. J.; Hughes, L. S.; Allen, J. O.; Cass, G. R. *Environ. Sci. Technol.* **1999**, *33*, 4331.

(9) Poi, C. A.; Lopes, D. A. *J. Geophys. Res.* **1998**, 103, 25263.

(10) Woods, D. C.; Chuan, R. L.; Rose, W. I. *Science* **1985**, *230*, 170.

(11) Hofmann, D. J.; Rosen, J. M. *Geophys. Res. Lett.* **1983**, *10*, 313.

(12) Allen, H. C.; Laux, J. M.; Finlayson-Pitts, B. J.; Hemminger, J. C. *J. Phys. Chem.* **1996**, *100*, 6371.

(13) De Haan, D. O.; Finlayson-Pitts, B. J. *J. Phys. Chem. A* **1997**, *101*, 9993.

(14) Jefferson, A.; Tanner, D. J.; Eisele, F. L.; Berresheim, H. *J. Geophys. Res.* **1998**, *103*, 1639.

(15) Laux, J. M.; Fister, T. F.; Finlayson-Pitts, B. J.; Hemminger, J. C. *J. Phys. Chem.* **1996**, *100*, 19891.

(16) Langer, S. R.; Pemberton, R. S.; Finlayson-Pitts, B. J. *J. Phys. Chem. A* **1997**, *101*, 1277.

10.1021/ja001469x CCC: $19.00

where many vibrational modes of simple inorganic molecules occur and from serious spectral interference from strong absorbers such as water.

Raman spectroscopy has been used in this laboratory for surface studies on NaCl based on its inherent molecular specificity, its immunity from spectral interference from water, and its routine accessibility to the low-frequency region of the spectrum. An added benefit to this approach is that it can easily be adapted to studies in a variety of atmospheric conditions. When combined with atomic force microscopy (AFM) to monitor surface morphological changes attendant to these reactions, considerable insight into this heterogeneous chemistry at an unprecedented level of molecular detail emerges. The power of these complementary techniques is demonstrated here for the study of the reaction of NaCl with H_2SO_4.

The nucleation, sources, and sinks of H_2SO_4 in the atmosphere have been extensively studied.[14,17] H_2SO_4 is extremely hygroscopic and its vapor pressure is 10^6 times lower than that of H_2O. Therefore, unlike other mineral acids, H_2SO_4 is found as a hydrated *liquid* in the atmosphere. The reaction of H_2SO_4 with NaCl has been proposed [5,18−21] to result in the formation of Na_2SO_4 with release of two moles of HCl per mole of H_2SO_4:

$$2NaCl\ (s) + H_2SO_4\ (l) \rightleftarrows 2HCl\ (g) + Na_2SO_4\ (s) \quad (1)$$

Analysis of atmospheric particles from the El Chichon eruption by energy-dispersive X-ray (EDX) spectroscopy showed the presence of a sulfur signal attributed to Na_2SO_4.[10] Although EDX spectroscopy is sensitive to the element of interest, it is insensitive to either the oxidation or protonation states of species from which the signals arise. Therefore, the chemical nature of the species from which these S signals arose cannot be determined. In more recent work, ten Brink studied the reaction of NaCl with H_2SO_4 in a smog chamber and found that the reaction kinetics were dependent on the size of the NaCl particle, but he was also unable to prove a Na_2SO_4 product.[19]

Understanding reaction pathways of atmospheric reactions is fundamental in the assessment of the chlorine budget. Although collection and analysis of atmospheric aerosols and particles provides information on the final products of such reactions, this information only leads to speculation about the relevant reaction mechanisms.

We have studied the reaction of NaCl with H_2SO_4 using Raman spectroscopy, a technique that allows direct interrogation of the products formed and their crystallographic phases. Mechanistic insight into the pathways by which these phases form on the NaCl surface can be ascertained from atomic force microscopy.

H_2O is ubiquitous in the terrestrial atmosphere and greatly affects the reaction probabilities of NaCl with NO_x species, but its effect on SO_x chemistry is unknown. Given the hygroscopic nature of H_2SO_4, atmospheric H_2SO_4 will be hydrated even at low relative humidities (RH). We have modeled this effect by exposing particulate NaCl to solutions of varying H_2O:H_2SO_4 ratios.

Models of this chemistry generally assume that all of the chlorine produced as HCl in this reaction is liberated to the atmosphere.[5,18−21] To better quantify the amount of HCl released, gravimetry was used to measure the amount of HCl liberated in H_2SO_4 solutions that model atmospheric aerosols at various RH.

Experimental Section

Materials. NaCl (Aldrich, >99.99%) was recrystallized from 50:50 H_2O:EtOH and heated at 550 °C for 72 h to remove surface H_2O. This scheme results in cubes with ~7 μm edges and a geometric surface area of ~4×10^3 cm^2/g. H_2SO_4 (Aldrich, >99.999%, 4 wt % H_2O) was added to powdered NaCl at a H_2SO_4:NaCl of 0.5:1 at ambient temperature and humidity (RH ranged from 7 to 25%). This experimental protocol ensures that H_2SO_4 is the limiting reagent. Aqueous samples of H_2SO_4 were prepared in sealed scintillation vials prior to analysis and added to powdered NaCl to ensure a H_2SO_4:NaCl of 0.5:1.

α-$NaHSO_4$ was prepared by heating $NaHSO_4 \cdot H_2O$ to 120 °C for 48 h. These samples did not absorb significant amounts of H_2O and did not undergo subsequent phase changes after exposure to ambient humidities for several weeks. β-$NaHSO_4$ was prepared in an evacuated flask by the addition of equal moles of Na_2SO_4 to 96 wt % H_2SO_4 at 130 °C with continual stirring for 12−24 h. The product was sealed in glass after synthesis and was verified by XRD and Raman spectroscopy.

Instrumentation. Raman spectra were acquired using 150 mW of 532 nm radiation from a Coherent Verdi 2 Nd:vanadate laser. A Minolta f/1.2 camera lens was used to collect scattered radiation at 90° with respect to the incident beam. A Spex 1877 Triplemate spectrometer coupled to a Princeton Instruments RTE-1100-PB thinned, back-illuminated CCD camera of 1100 × 330 pixel format cooled to −90 °C was used for Raman spectroscopy.

Contact mode AFM images were acquired using a Digital Instruments Multimode III SPM. A 1 × 1 cm^2 piece of NaCl (100) (International Crystal Laboratories) was cleaved in ambient (RH ~12%) prior to analysis. At these humidities, the NaCl (100) surface is covered with ca. 0.20 monolayer of H_2O.[22] An H_2SO_4 aerosol was generated by heating a solution of 96 wt % H_2SO_4 at ca. 120 °C in a sealed 1 cm diameter vial. The NaCl (100) was exposed to the aerosol by placing it over the heated vial for a prescribed period of time at 12% RH. During exposure, the NaCl crystal effectively covered the top of the vial, thereby preventing exposure of the solution to air. After exposure, the surface was immediately mounted in the AFM and images acquired in ambient.

Gravimetric experiments were performed using a Mettler Toledo AG204 Delta Range balance with 0.1 mg sensitivity. To ensure that NaCl was not the limiting reagent in these reactions, 2:1 NaCl:H_2SO_4 was used. Aqueous solutions of 0.1, 2, 4, and 8 H_2O:H_2SO_4 were prepared. Added to each vial was 1.07 ± 0.01 g of NaCl. Gravimetric measurements were made in capped 20 mL scintillation vials into which a 2 mm hole was drilled to allow HCl to escape. No significant mass loss (<1%) was recorded 24 h after exposure. This time is comparable to atmospheric lifetimes of NaCl aerosols in the troposphere,[1] and was used to determine the amount of HCl evolved from the reaction. The mass of each vial was determined initially, and then at a second time 24 h after addition of the H_2SO_4. Control samples of H_2O and NaCl were prepared to account for mass loss from H_2O evaporation. Ten replicate samples were acquired for each set of exposures.

Results and Discussion

Raman Spectroscopy. Differences in molecular symmetry between HSO_4^- and SO_4^{2-} result in distinct Raman spectra for different crystalline solids of the sodium salts.[23−25] As shown by the spectra in Figure 1 and the tabulated peak frequencies in Table 1, Na_2SO_4 has major bands at 467, 633, 994, and 1132 cm^{-1} while $NaHSO_4 \cdot H_2O$ has bands at 439, 606, 878, and 1042 cm^{-1}.[26−28] α-$NaHSO_4$ has clusters of major bands around 430 and 600 cm^{-1} with additional prominent bands at 869, 1006,

---

(17) Weber, R. J.; McMurry, P. H.; Mauldin, R. L.; Tanner, D. J.; Eisele, F. L.; Clarke, A. D.; Kapustin, V. N. *Geophys. Res. Lett.* **1999**, *26*, 307.

(18) Hitchcock, D. R.; Spiller, L. L.; Wilson, W. E. *Atmos. Environ.* **1980**, *14*, 165.

(19) ten Brink, H. M. *J. Aerosol Sci.* **1998**, *29*, 57.

(20) Jefferson, A.; Eisele, F. L.; Ziemann, P. J.; Weber, R. J.; Marti, J. J.; McMurry, P. H. *J. Geophys. Res.* **1997**, *102*, 19021.

(21) Symonds, R. B.; Rose, W. I.; Reed, M. H. *Nature* **1988**, *334*, 415.

(22) Peters, S. J.; Ewing, G. E. *Langmuir* **1997**, *13*, 6345.

(23) Choi, B.; Lockwood, D. J. *Solid State Commun.* **1989**, *72*, 133.

(24) Sonneveld, E. J.; Visser, J. W. *Acta Crystallogr.* **1979**, *B35*, 1975.

(25) Sonneveld, E. J.; Visser, J. W. *Acta Crystallogr.* **1978**, *B34*, 643.

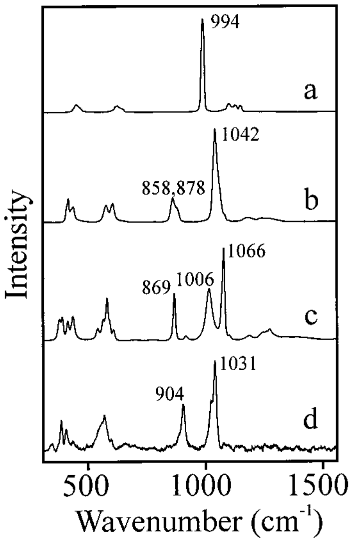

Figure 1. Raman spectra of bulk (a) Na_2SO_4, (b) $NaHSO_4 \cdot H_2O$, (c) anhydrous α-$NaHSO_4$, and (d) anhydrous β-$NaHSO_4$.

Table 1. Raman Frequencies of Sulfate Salts

peak freq (cm^{-1})				
α-$NaHSO_4$	β-$NaHSO_4$	$NaHSO_4 \cdot H_2O$	Na_2SO_4	assignment[a,b]
416	421	417		δ(S−O)
427				
447	439	439	451	δ(S−O)
469				
568	575	578		$\delta_s(SO_3)$
587	591			
605		606	613	$\delta_a(SO_3)$
630	617			
869	904	858		ν_s(S−O−H)
		878		
1006	1031	1042	981	ν_s(S−O)
1066				
1250	NO[c]	1243	1097	ν_a(S−O)
			1101	
			1152	

[a] Assignments for α-$NaHSO_4$, β-$NaHSO_4$, and $NaHSO_4 \cdot H_2O$ from refs 26, 27, and 28; assignment for Na_2SO_4 from ref 23. [b] δ = bend; ν = stretch; s = symmetric; a = asymmetric. [c] Not observed in these experiments.

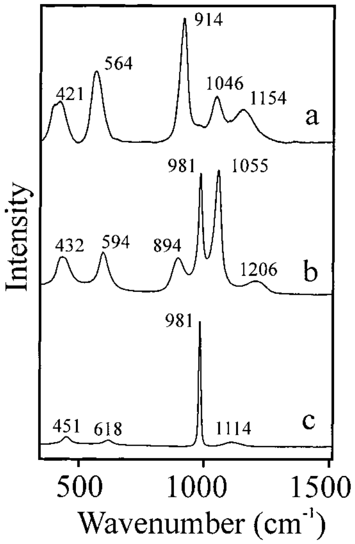

Figure 2. Solution Raman spectra of (a) 96 wt % H_2SO_4, (b) saturated aqueous $NaHSO_4 \cdot H_2O$, and (c) saturated aqueous Na_2SO_4.

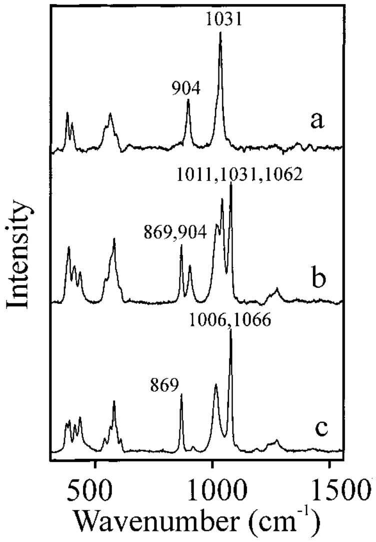

Figure 3. Raman spectra of 96 wt % H_2SO_4:NaCl at 0.5:1 after a reaction time of (a) 5 min, (b) 6 h, and (c) 24 h.

1066, and 1250 cm^{-1}.[28] β-$NaHSO_4$ has clusters of bands at ~430 and 580 cm^{-1} and additional major bands at 904 and 1031 cm^{-1}.[28]

The most intense peak in the spectra of all forms is the $\nu_s(SO_4)$. For Na_2SO_4, this mode is a sharp singlet at 994 cm^{-1}. In the spectrum of α-$NaHSO_4$, this mode is a doublet with peaks at 1006 and 1066 cm^{-1} due to the presence of two discrete HSO_4^- environments in the unit cell.[25,26] β-$NaHSO_4$ has a crystal structure in which all HSO_4^- are equivalent and exist in dimerized pairs.[25] Thus, the $\nu_s(SO_4)$ of β-$NaHSO_4$ occurs as a single peak at 1031 cm^{-1}. $NaHSO_4$ spectra have an additional band in the vicinity of 870−910 cm^{-1} due to the ν_s(S−O−H).

Raman spectra of aqueous SO_4^{2-} and HSO_4^- solutions are shown in Figure 2. These spectra have bands which are significantly broader than those in the spectra of the crystalline solids. The most intense mode in each spectrum is the $\nu_s(SO_4)$,[29] which appears at 914 cm^{-1} in 96 wt % H_2SO_4, shown in Figure 2a. The spectrum of a saturated aqueous solution of $NaHSO_4 \cdot H_2O$ shown in Figure 2b has two intense modes at 981 and 1055 cm^{-1} which are assigned to the $\nu_s(SO_4)$ of SO_4^{2-} and HSO_4^-, respectively.[29] The solution of saturated Na_2SO_4 is dominated by the $\nu_s(SO_4)$ at 981 cm^{-1}.

Raman spectra were acquired with time after exposure of powdered NaCl to 96 wt % H_2SO_4 at a H_2SO_4:NaCl ratio of 0.5:1 at 25% RH. The spectra shown in Figure 3a−c represent spectra of the reaction products 5 min, 6 h, and 24 h after reaction, respectively. These spectra reflect a slow, systematic change in NaCl surface product over this period. None of these spectra is consistent with the presence of Na_2SO_4, the previously assumed[5,18−21] product of this reaction. Instead, the observation of a $\nu_s(SO_4)$ mode at frequencies greater than 1000 cm^{-1} suggests a $NaHSO_4$ product. The observation of a distinct v_s(S−O−H), initially at 904 cm^{-1} but shifting to 869 cm^{-1} with time, is further consistent with $NaHSO_4$.

The spectrum in Figure 3a for the reaction product formed immediately after exposure of NaCl to H_2SO_4 does not match that of either α-$NaHSO_4$ or $NaHSO_4 \cdot H_2O$ as shown in Figure 1, spectra b and c, respectively. In contrast, the spectrum in

---

(26) Dey, B.; Jain, Y. S.; Verma, A. L. *J. Raman Spectrosc.* **1982**, *13*, 209.

(27) Goypiron, A.; de Villepin, J.; Novak, A. *J. Raman Spectrosc.* **1980**, *9*, 297.

(28) Baran, J.; Ilczszyn, M. M.; Marchewka, M. K.; Ratajczak, H. *Spectrosc. Lett.* **1999**, *32*, 83.

(29) Irish, D. E.; Chen, H. *J. Phys. Chem.* **1970**, *74*, 3796.

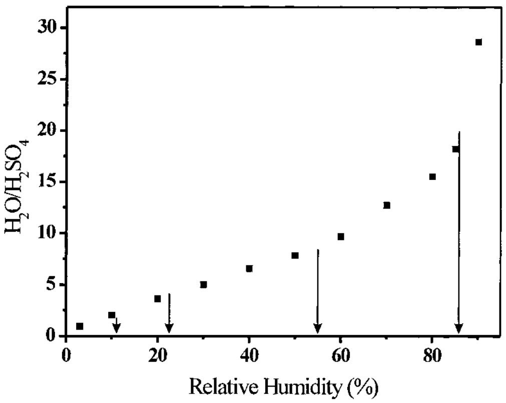

Figure 4. $H_2O:H_2SO_4$ as a function of RH (neglecting the Kelvin effect). Arrows indicate RH values modeled in this study.

Figure 3a can be attributed to β-$NaHSO_4$, a relatively unstable form of $NaHSO_4$.[25,28]

Previous researchers have reported considerable difficulty in isolating pure β-$NaHSO_4$ in the presence of gas-phase moisture.[25] Indeed, we have recently confirmed that H_2O catalyzes the transformation of pure bulk β-$NaHSO_4$ to α-$NaHSO_4$.[30] The same transformation occurs for NaCl surface-confined β-$NaHSO_4$ formed in the reaction with H_2SO_4. Within 10 min of H_2SO_4 exposure, the ν_s(S−O−H) at 904 cm^{-1} decreases in intensity at the expense of a new ν_s(S−O−H) at 869 cm^{-1} (Figure 3b,c). Growth of two new $\nu_s(SO_4)$ modes at 1011 and 1062 cm^{-1} at the expense of that at 1031 cm^{-1} is also consistent with the transformation from β-$NaHSO_4$ to α-$NaHSO_4$.

This transformation takes ~15−18 h at the relative humidities (7−25%) used in this study. Given that the atmospheric lifetime of NaCl particles is on the order of 6−24 h depending on size, these changes may manifest themselves on atmospheric particles prior to deposition.

Several experiments were also undertaken in which powdered NaCl was exposed to H_2SO_4 by passing a stream of aerosol droplets created by evacuation of 96 wt % H_2SO_4 over the NaCl. This experimental arrangement better reflects the exact nature of atmospheric exposure of NaCl to H_2SO_4 which exists as aerosol droplets. The spectral results indicate the formation of α-$NaHSO_4$ after ~ 48 h of H_2SO_4 aerosol exposure (data not shown). β-$NaHSO_4$ was not observed, probably due to small amounts of H_2O vapor in the headspace which cause the phase transition on this time scale.

H_2SO_4 that is 96 wt % has a $H_2O:H_2SO_4$ ratio of 1:9. This composition is a poor model for H_2SO_4 in the terrestrial atmosphere where the water content is much higher. The hydration of H_2SO_4 in the atmosphere depends on RH; several stable hydrates of H_2SO_4 are known to form.[31] Figure 4 shows a plot of the $H_2O:H_2SO_4$ ratio in these hydrates at 298 K as a function of RH[1,32] (neglecting the Kelvin effect.) The hydration of H_2SO_4 increases linearly between a RH of 0 and 70%. Above this point, the hydration number increases exponentially to nearly 30 at ~80% RH.

To model environments of 10, 22, 55, and 85% RH, solutions of 2:1, 4:1, 8:1, and 20:1 $H_2O:H_2SO_4$ mixtures, respectively, were prepared. These compositions were chosen because they have been shown to be thermodynamically stable H_2SO_4 hydrates,[31] and they model a range of humidities in the terrestrial atmosphere. In fact, the hydrate formed in the 4:1 mixture has been observed in the atmosphere.[33] RH data from coastal sites within the United States were obtained from the National Weather Service (NWS) and National Oceanic and Atmospheric Administration (NOAA).[34] The 24 h average RH obtained from 77 coastal sites located in the United States and its territories is 73 ± 11%. Assuming that the evaporation of sea salt aerosols occurs in proximity to the coast, one would predict that H_2SO_4 exists as an aqueous aerosol with a composition of 20:1. Thus, these compositions, particularly those of the hydrates with larger amounts of H_2O, are atmospherically relevant in the marine boundary layer.

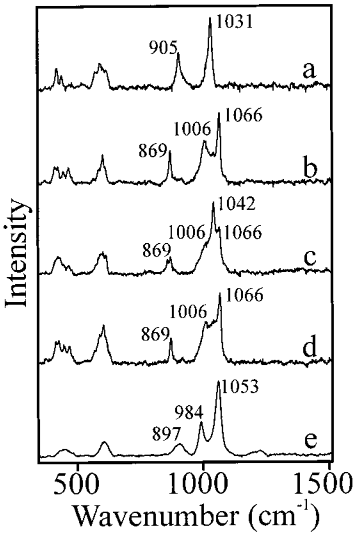

Figure 5. Raman spectra of NaCl after reaction with (a) 2 $H_2O:H_2SO_4$, (b) 4 $H_2O:H_2SO_4$, (c) 8 $H_2O:H_2SO_4$, (d) 8 $H_2O:H_2SO_4$ after 24 h, and (e) 20:1 $H_2O:H_2SO_4$.

Spectra of the products formed by the exposure of powdered NaCl to H_2SO_4 solutions such that the final mixtures possessed compositions of $NaCl:H_2O:H_2SO_4$ of 2:2:1, 2:4:1, 2:8:1, and 2:20:1 are shown in Figure 5. Each spectrum was acquired ~15 min after exposure to the H_2SO_4 solution. The reaction of NaCl with a 2:1 $H_2O:H_2SO_4$ solution results in the formation of α-$NaHSO_4$ as shown by the spectrum in Figure 5a. However, after 24 h, this β-$NaHSO_4$ has undergone transformation to α-$NaHSO_4$.

The Raman spectrum in Figure 5b shows the product of exposing NaCl to 4:1 $H_2O:H_2SO_4$ to be α-$NaHSO_4$ based on the frequencies of the $\nu_s(SO_4)$ doublet at 1006 and 1066 cm^{-1}. In addition, the weak $\nu_s(SO_4)$ at 1042 cm^{-1} is consistent with the formation of a small amount of $NaHSO_4 \cdot H_2O$. This product is a solid that is visibly wet. Spectroscopic evidence for the presence of surface H_2O is the shoulder at 981 cm^{-1} which is attributed to aqueous HSO_4^- species as shown by the spectrum of saturated $NaHSO_4 \cdot H_2O$ solution in Figure 2b. Spectra taken 24 h after exposure to this H_2SO_4 hydrate (not shown) indicate the loss of the $\nu_s(SO_4)$ mode of $NaHSO_4 \cdot H_2O$ at 1042 cm^{-1} indicating the conversion of all $NaHSO_4 \cdot H_2O$ to anhydrous α-$NaHSO_4$. Given that this sample is a highly viscous slurry, the transformation to a completely anhydrous bisulfate product is surprising.

Exposure of NaCl to 8:1 $H_2O:H_2SO_4$ yields the spectrum shown in Figure 5c. The bands at 1006, 1042, and 1066 cm^{-1}

---

(30) Zangmeister, C. D.; Pemberton, J. E. *J. Solid State Chem.* Submitted for publication.

(31) Giaque, W. F.; Hornung, E. W.; Kunzler, J. E.; Rubin, T. R. *J. Am. Chem. Soc.* **1959**, *82*, 62.

(32) Liu, B. Y. H.; Levi, J. In *Generation of Aerosols and Facilities for Exposure Experiments*; Willeke, K., Ed.; Ann Arbor Science: Ann Arbor, MI, 1980; pp 317−336.

(33) Sassen, K.; Peter, T.; Luo, B. P.; Crutzen, P. J. *Appl. Opt.* **1994**, *33*, 4602.

(34) Obtained from relative humidity data collected by the National Oceanographic and Atmospheric agency (NOAA) and the National Weather Service (NWS) from http://met-www.cit.cornell.edu/ccd/relhum98.html.

are consistent with the presence of both α-$NaHSO_4$ and $NaHSO_4 \cdot H_2O$. The partial dissolution of solid $NaHSO_4$ is more evident in the 8:1 sample as shown by the more pronounced presence of the solution HSO_4^- 981 cm^{-1} mode. Spectra taken 24 h after exposure (Figure 5d) indicate a dramatic reduction in the amount of $NaHSO_4 \cdot H_2O$ at the expense of an increase in α-$NaHSO_4$ modes.

To simulate 85% RH, a 20:1 H_2O:H_2SO_4 solution was prepared. This sample contains ~10 mol of H_2O per mol of NaCl. Thus, this sample contains sufficient H_2O to entirely dissolve the solid. The Raman spectrum shown in Figure 5e is of the resulting solution product. This spectrum is similar to that of saturated aqueous $NaHSO_4$ shown in Figure 2b. However, the intensity of the 984 cm^{-1} mode of solution SO_4^{2-} is less intense relative to the 1053 cm^{-1} mode of solution HSO_4^- reflecting a lower solution pH than in saturated aqueous $NaHSO_4$. This lower pH is the result of HCl production in this reaction. Assuming total conversion of NaCl to $NaHSO_4$, the HCl concentration in this solution is ~1.4 M, although Brimblecombe et al.[35] have shown that HCl degassing is thermodynamically favored at pH <3. Therefore, the initial HCl generated from this reaction is degassed until the equilibrium value of pH ~3 is reached, a pH at which partial SO_4^{2-} protonation to HSO_4^- is favored.

The presence of H_2O in the H_2SO_4 does not change the product of the NaCl reaction from $NaHSO_4$; however, the phase of anhydrous $NaHSO_4$ formed depends on the amount of H_2O available for hydration of the sample. It is possible to form $NaHSO_4 \cdot H_2O$ at large relative amounts of H_2O. However, the $NaHSO_4 \cdot H_2O$ is not stable on the NaCl surface and loses H_2O to become the anhydrous α-$NaHSO_4$ phase over the course of 24 h. The loss of $NaHSO_4 \cdot H_2O$ with the concomitant growth of α-$NaHSO_4$ may be due to hydration of NaCl at the expense of HSO_4^-. The crystallographic rearrangement required for such a transformation must be kinetically slow, and thus require up to ~24 h to achieve equilibrium. It is unlikely that H_2O evaporation results in the observed changes, as the samples were kept tightly sealed between and during sample acquisitions.

The apparent desiccating effect of NaCl in this system suggests greater affinity for H_2O by NaCl than by α-$NaHSO_4$. Given that the deliquescence points (DP) of NaCl and $NaHSO_4 \cdot H_2O$ are 74.5% and 52%, respectively,[1] this observation may seem somewhat surprising. However, in this system, it is the relative affinity of H_2O by NaCl and α-$NaHSO_4$ that is relevant, and since the DP of α-$NaHSO_4$ cannot be determined due to its conversion to $NaHSO_4 \cdot H_2O$, this relative affinity cannot be known. Based on the observation that NaCl takes H_2O from $NaHSO_4 \cdot H_2O$ on its surface, one must conclude that either the presence of the NaCl surface raises the DP of $NaHSO_4 \cdot H_2O$ above that of NaCl or the DP of α-$NaHSO_4$ is higher than that of either NaCl or $NaHSO_4 \cdot H_2O$. The atmospheric relevance of these observations is that the presence of unexpected products in such reactions may significantly alter the expected uptake of H_2O by solid particles.

Unlike the reaction of NaCl with HNO_3 and NO_2,[13] a thin passivating surface layer of the reaction product is not observed in this reaction. The species present in this study (NaCl and $NaHSO_4$) are optically transparent at the excitation wavelength used; therefore, the sampling depth is large and extends much beyond the surface into the bulk. Indeed, the sampling depth may exceed the mean powder size (~7 μm) depending on scattering. The signal arising from the surface of the sample is much less than the Raman scattering from the bulk. Thus, spectral contributions from processes such as surface deliquescence are not observed in this study.

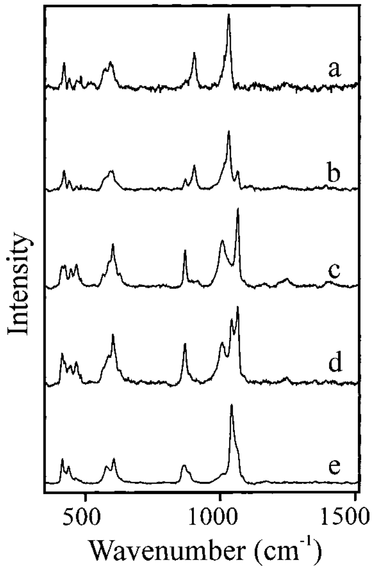

Figure 6. Raman spectra of β-$NaHSO_4$ on NaCl exposed to 100% RH. Spectra of (a) β-$NaHSO_4$ prior to exposure, (b) mixture of β-$NaHSO_4$ and α-$NaHSO_4$ 10 min after exposure, (c) pure α-$NaHSO_4$ 20 min after exposure, (d) mixture of $NaHSO_4 \cdot H_2O$ and α-$NaHSO_4$ 30 min after exposure, and (e) pure $NaHSO_4 \cdot H_2O$ 40 min after exposure.

To further study the effect of H_2O on the phase transition of anhydrous β-$NaHSO_4$ to α-$NaHSO_4$, several samples of NaCl were exposed to 96 wt % H_2SO_4 (0.5:1 H_2SO_4:NaCl) in a dry bag and stored in a desiccator for several days. Spectra of these samples indicate the initial formation of pure β-$NaHSO_4$ in this dry environment. Even after 4 days, the β-$NaHSO_4$ formed in this reaction is stable if it is kept dry as indicated by the spectrum in Figure 6a.

Exposure of this 1:1 β-$NaHSO_4$:NaCl sample to an environment of 100% RH produces the sequence of spectra shown in Figure 6b–e. Figure 6b was acquired ~10 min after exposure to the 100% RH environment and indicates growth of the α-$NaHSO_4$ phase. Further exposure to 100% RH results in the spectrum shown in Figure 6c. At this point, nearly all of the β-$NaHSO_4$ has been converted to α-$NaHSO_4$. As this powder is continually exposed to 100% RH, the $\nu_s(SO_4)$ mode of $NaHSO_4 \cdot H_2O$ at 1042 cm^{-1} appears as shown in Figure 6d. Figure 6e was acquired ~30 min after Figure 6b; at this point, the conversion of α-$NaHSO_4$ to $NaHSO_4 \cdot H_2O$ is complete. Very little spectral evidence for the presence of solution phase species exists in Figure 6b–e. This absence may be due to the fast uptake of H_2O by α-$NaHSO_4$ to form $NaHSO_4 \cdot H_2O$ and/or a α-$NaHSO_4$ DP greater than the 52% DP of $NaHSO_4 \cdot H_2O$.

Collectively, these results clearly indicate that the presence of H_2O catalyzes the transformation of anhydrous β-$NaHSO_4$ to anhydrous α-$NaHSO_4$. H_2O-mediated phase transitions have been observed for other HSO_4^- salts;[36-39] however, this is the first such observation for $NaHSO_4$. Careful inspection of the crystal structures of these three phases indicates that those of α-$NaHSO_4$ and $NaHSO_4 \cdot H_2O$ are similar[25,28] with each having two discrete HSO_4^- environments per unit cell.[24,28] We speculate

---

[35] Brimblecombe, P.; Clegg, S. L. *J. Atmos. Chem.* **1988**, *7*, 1.

[36] Baranowski, B.; Lipkowski, J.; Lundén, A. *J. Solid State Chem.* **1995**, *117*, 412.

[37] Baranowski, B.; Friesel, M.; Lundén, A. *Z. Naturforsch.* **1987**, *42A*, 565.

[38] Baranowski, B.; Friesel, M.; Lundén, A. *Z. Naturforsch.* **1986**, *41A*, 981.

[39] Colomban, Ph.; Pham-Thi, M.; Novak, A. *Solid State Ionics* **1987**, *24*, 193.

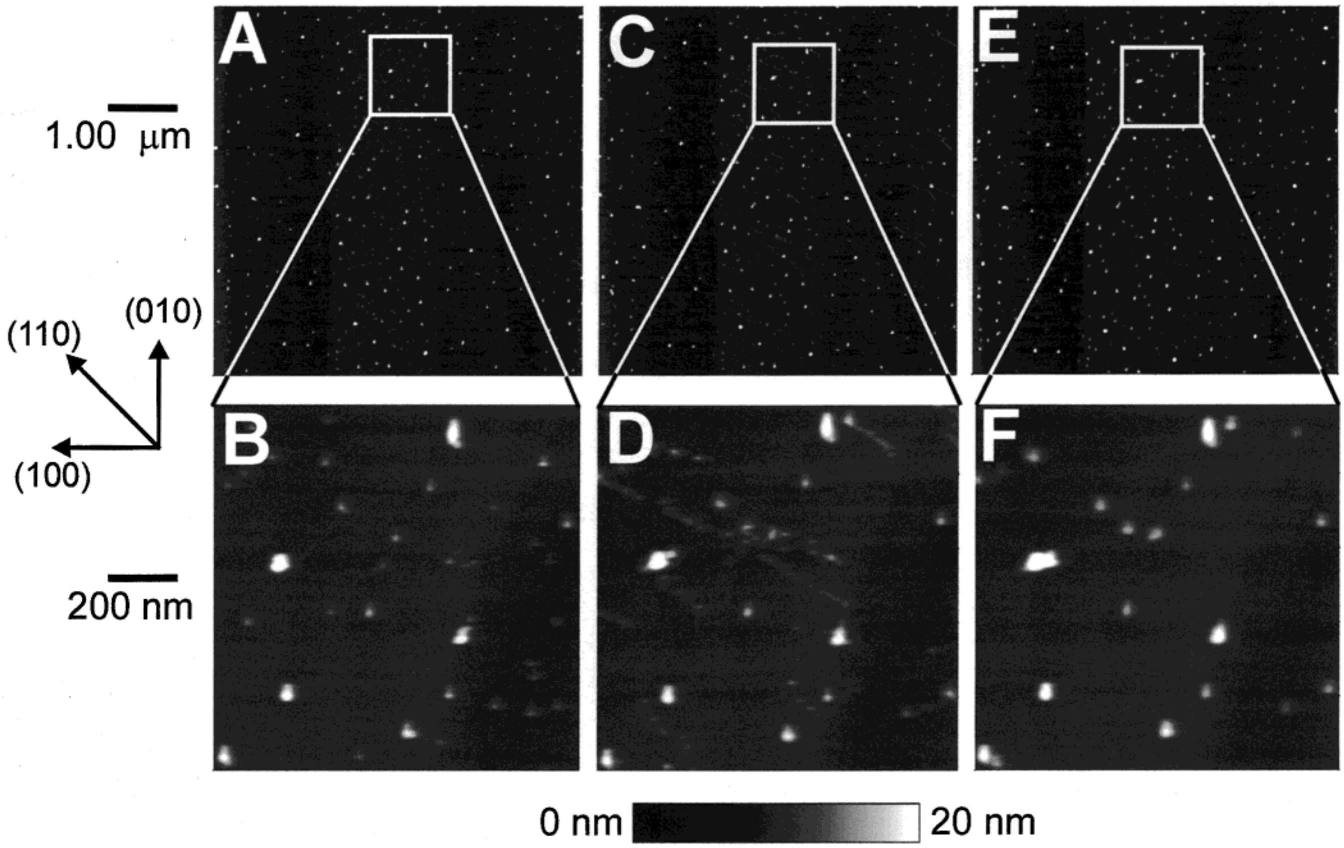

Figure 7. Contact AFM images after exposure of NaCl (100) to H_2SO_4 aerosol: (a, b) images 4 min after exposure; (c, d) images 12 min after exposure; (e, f) images 20 min after exposure; (a, c, and e) 5 × 5 μm^2 region; (b, d, and f) 1 × 1 μm^2 region.

that the phase transition from β-$NaHSO_4$ to α-$NaHSO_4$ is initiated by hydration of Na^+ in the β phase. Exposure to higher RH results in the incorporation of H_2O into the crystal structure to form $NaHSO_4{\cdot}H_2O$. We have recently proven that the β-$NaHSO_4$ to α-$NaHSO_4$ phase transition also occurs in the absence of NaCl, but much more slowly.[30] Thus, one can speculate that NaCl facilitates H_2O uptake, thereby increasing the rate of the phase transition.

Atomic Force Microscopy. Further insight into the initial stages of this reaction comes from AFM on NaCl (100) surfaces exposed to H_2SO_4 aerosols. The average diameters of airborne H_2SO_4 aerosol droplets and NaCl particles have been estimated to be ~1 and 5 μm, respectively.[1] Thus, to create an atmospherically relevant model of the interaction of H_2SO_4 aerosols with the surfaces of NaCl particles, H_2SO_4 droplets that are smaller than the NaCl surface are desired. Such an aerosol population was achieved by heating 96 wt % H_2SO_4 in a closed vial at 120 °C at 12% RH. Based on the data in Figure 4, these H_2SO_4 aerosols are assumed to be composed of ~3:1 H_2O:H_2SO_4. Subsequent handling and mounting of the NaCl crystal after exposure takes additional time. Thus, scanning was initiated ~4 min after exposure of the NaCl surface to these H_2SO_4 aerosols. It should also be noted that the surface was exposed to 12% RH during the entire exposure and AFM analysis sequence.

A series of real-time contact mode AFM images collected in one region of the surface over 16 min is shown in Figure 7. Vertical stripes that run down the length of the images in Figure 7a,c,e are monatomic steps on the NaCl surface. A uniform distribution of reaction products is observed that is consistent with reaction of aerosol droplets with the NaCl surface.

After 5 min of H_2SO_4 aerosol exposure (Figure 7b), stationary, pyramidal-shaped structures that are separated by ~100 nm form at step edges and on terrace sites. Assuming that these structures are $NaHSO_4$, their size and aspect ratio provide insight into which phase they represent. The dimensions of these structures are 55.7 ± 8.0 nm × 58.9 ± 12.7 nm (x−y aspect ratio of 1.1 ± 0.1) with an average height of ~20 nm. This ratio compares favorably to the 1.15 b/c aspect ratio of α-$NaHSO_4$ as shown by the crystallographic data in Table 2.[25] Thus, based on this aspect ratio and the Raman spectral data of this reaction shown in Figure 3c, these structures are proposed to be α-$NaHSO_4$.

Table 2. Unit Cell Dimensions of Anhydrous $NaHSO_4$ Phases

	unit cell parameters[a]		
phase	a (Å)	b (Å)	c (Å)
α-$NaHSO_4$	7.005	7.125	6.172
β-$NaHSO_4$	8.759	7.500	5.147

[a] References 24 and 25.

In addition to these α-$NaHSO_4$ particles, a large population of smaller structures (6−8 times as many as the α-$NaHSO_4$ particles) is also observed on the surface. In Figure 7a,b, these structures have dimensions of 12.9 ± 1.9 nm × 22.4 ± 3.2 nm (x−y aspect ratio of 1.7 ± 0.2) with an average height of 2.5 nm. This aspect ratio compares favorably to the 1.70 a/c aspect ratio of β-$NaHSO_4$ as shown in Table 2.[24] On the basis of this aspect ratio and the Raman spectral data shown in Figure 3a, these smaller structures are proposed to be β-$NaHSO_4$.

Continuous scanning of the same surface region results in the images shown in Figure 7c−f. In Figure 7c,d, many of the smaller β-$NaHSO_4$ structures are observed to be mobile across the surface. These β-$NaHSO_4$ structures disappear from the surface by the next scan (Figure 7e taken ~4 min later) and the nearby α-$NaHSO_4$ structures are larger in Figure 7e than in

Figure 7a. The β-$NaHSO_4$ structures are mobile and move at 45° with respect to the NaCl (100) plane, or in other words, along the NaCl (110) plane. Motion of β-$NaHSO_4$ along the NaCl (110) direction must represent the lowest energy plane of motion. This movement can be rationalized by realizing that the *a*/*c* plane of β-$NaHSO_4$ has Na^+ in the plane[24,25] coincident with the NaCl surface that allows movement along a single row of Na^+ without encountering Cl^- as would occur for movement along the NaCl (100) plane.

The movement of β-$NaHSO_4$ ceases over the 16 min that span the data in Figure 7. The encounter of β-$NaHSO_4$ with α-$NaHSO_4$ results in coalescence of the two structures. As a result, the α-$NaHSO_4$ structures increase in size while still retaining their 1.1 ± 0.1 aspect ratio.

In some cases, movement of the β-$NaHSO_4$ structures results in encounters with a step edge before an existing particle of α-$NaHSO_4$. In ~95% of such cases, the β-$NaHSO_4$ structures at the step edge coalesce and transform into a single α-$NaHSO_4$ structure based on their aspect ratios. This transformation is probably the result of the presence of H_2O, which collects preferentially at the step edges,[40] that mediates this transformation as noted above. The remaining 5% of these encounters result in crossing of the step edge by the β-$NaHSO_4$ and continued movement along the NaCl (110) plane.

β-$NaHSO_4$ surface translation is hypothesized to be promoted either by dissolution and reprecipitation of $NaHSO_4$ or cation–anion place exchange along the (110) plane. H_2O has been observed to facilitate the rearrangement of soluble surfaces in previous work,[40,41] and may be responsible for surface translation in this study. Since H_2O initiates the phase transition from β- to α-$NaHSO_4$, any $NaHSO_4$ that was to reprecipitate would be α-$NaHSO_4$. Thus, dissolution and reprecipitation is not a feasible mechanism for translation of β-$NaHSO_4$, leaving the ion place exchange as the most likely translation mode. H_2O may aid this place exchange by dissolution of the NaCl surface during the process.

The transformation of anhydrous β-$NaHSO_4$ to α-$NaHSO_4$ is mediated by H_2O and the rate at which the transition takes place on the NaCl surface is greatly influenced by the RH. This observation explains the difference in time for the phase transition as monitored by Raman spectroscopy in a closed environment as compared to that monitored in the ambient AFM experiments. By carefully controlling the amount of H_2O in these experiments, the phase transition can be totally eliminated for up to several days.

Gravimetry of HCl Release. The hygroscopic nature of H_2SO_4 ensures that the acid is always hydrated in the earth's atmosphere. The presence of water may have two effects in the reaction of NaCl with H_2SO_4. First, H_2O might increase the kinetics of the reaction as has been observed in the reaction of NaCl with nitrogen oxide species.[13] In addition, H_2O may also sequester the HCl produced in this reaction by dissolution. Thus, the amount of HCl that is released into the atmosphere may be considerably less than that produced in the reaction. Previous studies on the release of atmospherically relevant gas-phase acids in solution have been undertaken.[35,42] However, these studies were confined to reactions that occur in droplets or solution. The work reported here is the first such study of the release of surface-confined HCl from a H_2O-limited environment.

To determine the mass of HCl released as a function of the H_2O content of the H_2SO_4, a series of gravimetric experiments were performed in which the total system mass was monitored before reaction and after reaction and equilibration of the products with the surrounding atmosphere in an open vessel. Once reaction and equilibration had occurred, no further mass changes were noted for periods up to 24 h. The significance of these experiments is that they represent the first studies done under tropospherically relevent pressures. Previous studies of HCl release[18] have been performed in vacuum environments which facilitate removal of the HCl formed in the reaction. These previous experiments performed under vacuum[19] might be expected to provide results different from those that occur at tropospheric pressures.

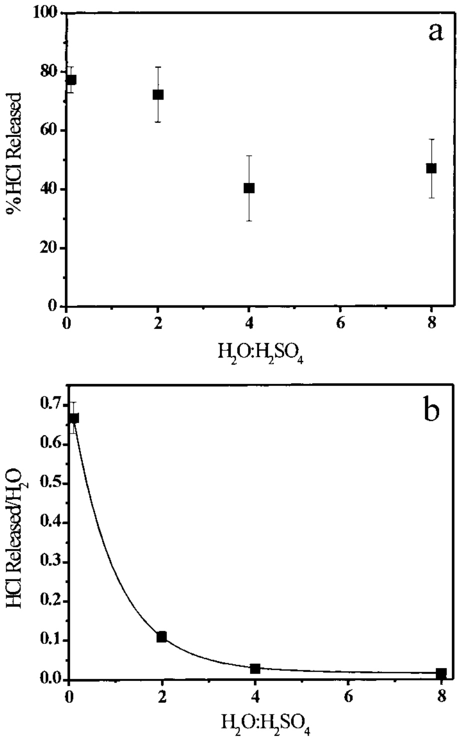

Figure 8. (a) Percent HCl released from NaCl surface as a function of $H_2O:H_2SO_4$; (b) HCl release per H_2O as a function of $H_2O:H_2SO_4$.

Table 3. Gravimetric Results for HCl Evolution as a Function of $H_2O:H_2SO_4$

$H_2O:H_2SO_4$ soln	% RH simulated[a]	% HCl lost of total HCl produced[b]
0.1:1	<1	77.4 ± 4.5
2:1	10	72.6 ± 9.4
4:1	22	40.2 ± 11.1
8:1	55	46.8 ± 9.9

[a] References 1, 31,and 32. [b] Based on mass loss over 24 h.

Four aqueous solutions of H_2SO_4 were prepared with $H_2O:H_2SO_4$ of 0.1, 2, 4, and 8. These solutions were added to powdered NaCl in a 2:1 $NaCl:H_2SO_4$ solution ratio. The reactions in 0.1 and 2 $H_2O:H_2SO_4$ solutions produce solid products, whereas those in 4 and 8 $H_2O:H_2SO_4$ solutions result in products containing both solid and liquid phases. The percent HCl released from the solid product as a function of $H_2O:H_2SO_4$ is shown in Figure 8a and tabulated in Table 3. These results indicate that the solid products release ~30% more HCl than the mixture of solid and liquid-phase products.

The effect of the presence of H_2O on the release of HCl from the solid products is pronounced. As shown in Figure 8b, ~0.68 HCl per H_2O is released for 0.1 $H_2O:H_2SO_4$. This value drops to 0.12 HCl per H_2O at 2 $H_2O:H_2SO_4$ and further decreases to 0.025 for 4 and 8 $H_2O:H_2SO_4$. Thus, as the amount of H_2O in

---

(40) Dui, Q.; Hu, J.; Salmeron, M. *J. Phys. Chem. B* **1997**, *101*, 1994.
(41) Zangmeister, C. D.; Pemberton, J. E. *J. Phys. Chem. B* **1998**, *102*, 8950.
(42) Clegg, S. L.; Brimblecombe, P. *Atmos. Environ.* **1988**, *22*, 91.

the H_2SO_4 increases, the amount of HCl released decreases as there is more H_2O available for dissolution of the HCl produced. Atmospherically, dissolution of HCl may significantly decrease the amount of HCl released at humidities greater than ~30%. In light of the work by Brimblecombe and Clegg on bulk aqueous solutions,[35,42] these results are not too surprising. However, the significance of these observations lies in the fact that the behavior observed in ultrathin H_2O films on NaCl is essentially identical to that observed in bulk aqueous solutions.

Atmospheric Relevance. The El Chichon volcanic eruption generated $\sim 3 \times 10^7$ molecules of 60−80 wt % H_2SO_4 per cm^{-3} [11] and 5.2×10^9 molecules of particulate NaCl per cm^{-3} in the stratosphere.[43] Furthermore, recent work has shown that H_2SO_4 aerosols exist in the liquid state at stratospheric temperatures.[44−46] Considering the number density of the each of the reactants, the release of HCl from the reaction of NaCl with H_2SO_4 aerosols is likely at these high altitudes.

The loss of Cl^- from sea salt particles has been measured at many sites across the earth's surface.[5−9] For example, Poi et al. observed at a site in Portugal Cl^- depletions greater than 85%, with a depletion rate of 10% Cl^- per h.[9] In such an atmosphere, SO_2 levels, a H_2SO_4 precursor,[47] are 4.3 times greater than those of NO_2 and 5.7 times higher than those of HNO_3.[9] Thus, the extent of the NaCl reaction with H_2SO_4 may also be high in such an environment. The formation of only 1 mol of HCl per mol of H_2SO_4 reduces the impact of this reaction on the generation of chlorine reservoir species.

Conclusions

The reaction of NaCl with H_2SO_4 has been investigated as a function of H_2O content using Raman spectroscopy, AFM, and gravimetric analysis. The product formed is $NaHSO_4$, not Na_2SO_4 as previously proposed, and is independent of H_2O content. The initial product formed is anhydrous β-$NaHSO_4$ which undergoes an H_2O-mediated phase transition to the anhydrous α-$NaHSO_4$ phase. The kinetics of this transition are extremely sensitive to RH.

The β- to α-$NaHSO_4$ phase transition is also observed using AFM on NaCl (100). Exposure of NaCl (100) to H_2SO_4 produces $NaHSO_4$ structures with aspect ratios consistent with β-$NaHSO_4$. These species are mobile on the NaCl (100) surface, moving exclusively along the (110) plane. Encounter of these β-$NaHSO_4$ structures with an existing α-$NaHSO_4$ structure or a step edge leads to their transformation to α-$NaHSO_4$.

Gravimetric analysis of the reaction of NaCl with H_2SO_4 indicates that the amount of HCl released is dependent on the amount of H_2O available for dissolution of the product. The fraction of HCl released is reduced at high RH by up to ~40%.

Acknowledgment. The authors gratefully acknowledge the National Science Foundation (CHE-9504345 and CHE-0075813) for financial support of this research.

JA001469X

---

(43) Michelangeli, D. V.; Allen, M.; Yung, Y. L. *Geophys. Res. Lett.* **1991**, *18*, 673.

(44) Bertram, A. K.; Patterson, D. D.; Sloan, J. J. *J. Phys. Chem.* **1996**, *100*, 2376.

(45) Martin, S. T.; Salcedo, D.; Molina, L. T.; Molina, M. J. *J. Phys. Chem. B* **1997**, *101*, 5307.

(46) Koop, T.; Ng, H. P.; Molina, L. T.; Molina, M. J. *J. Phys. Chem. A* **1998**, *102*, 8924.

(47) Jefferson, A.; Tanner, D. J.; Eisele, F. L.; Berresheim, H. *J. Geophys. Res.* **1998**, *103*, 1639.